

# LHC constraints on Yukawa unification in SO(10)

Marcin Badziak<sup>a,b,1</sup>, Kazuki Sakurai<sup>c2</sup>

<sup>a</sup>*Department of Applied Mathematics and Theoretical Physics, Centre for Mathematical Sciences, University of Cambridge, Wilberforce Road, Cambridge CB3 0WA, United Kingdom*

<sup>b</sup>*Cavendish Laboratory, University of Cambridge, J.J. Thomson Avenue, Cambridge CB3 0HE, United Kingdom*

<sup>c</sup>*Deutsches Elektronen Synchrotron DESY, Notkestrasse 85, D-22607 Hamburg, Germany*

## Abstract

LHC constraints on the recently proposed SUSY SO(10) GUT model with top-bottom-tau Yukawa unification are investigated. In this model, various phenomenological constraints are in concord with Yukawa unification thanks to the negative sign of  $\mu$ ,  $D$ -term splitting in the soft scalar masses and non-universal gaugino masses generated by non-zero  $F$ -term in a 24-dimensional representation of  $SU(5) \subset SO(10)$ . After discussing the impact of the CP-odd Higgs boson mass bound on this model, we provide a detailed analysis of the recent direct SUSY searches performed by ATLAS and investigate the constraints on this SO(10) model. At 95% confidence level, the lower limit on the gluino mass is found at 675 GeV. Assuming an integrated luminosity of  $10 \text{ fb}^{-1}$ , this bound may be extended to 1.1 TeV if the right-handed down squark is lighter than about 1 TeV.

---

<sup>1</sup>M.Badziak@damtp.cam.ac.uk

<sup>2</sup>kazuki.sakurai@desy.de

# 1 Introduction

In the simplest versions of supersymmetric (SUSY) Grand Unified Theories (GUTs) based on SO(10) gauge symmetry, in which the Minimal Supersymmetric Standard Model (MSSM) Higgs doublets,  $H_u$  and  $H_d$ , reside in a **10** of SO(10), Yukawa couplings of top, bottom and tau unify at the GUT scale. Unlike the gauge coupling unification, Yukawa coupling unification is very sensitive to weak scale threshold corrections which depend on the entire SUSY spectrum [1, 2, 3]. Moreover, top-bottom-tau Yukawa unification is often in conflict with radiative electroweak symmetry breaking (REWSB) [2]. Therefore, the condition of top-bottom-tau Yukawa unification at the GUT scale impose non-trivial constraints on soft SUSY breaking terms. In particular, it has been shown that Yukawa unification is incompatible with REWSB in the Constrained MSSM (CMSSM) where the soft masses for scalars and gauginos are universal at the GUT scale [2].

SO(10) models are rather constrained not only because of the requirement of Yukawa unification but also due to their ability to fit all the MSSM sfermions of each generation into a single **16** of SO(10). Thus, assuming the Minimal Flavor Violation [4, 5], the only non-universality in the scalar masses consistent with SO(10) gauge symmetry is the mass splitting between sfermions and Higgses. This has been shown to be insufficient to make Yukawa unification compatible with REWSB [6]. However, if SO(10) gauge symmetry is spontaneously broken, as is generally expected, in the effective theory below the GUT scale generic  $D$ -term contribution splits the scalar masses residing in the same representation of SO(10) [7]. Most importantly,  $D$ -term contribution splits masses of the MSSM Higgs doublets and may lead to Yukawa unification consistent with REWSB [8].

Requirement of top-bottom-tau Yukawa unification prefers negative values of the Higgs-mixing parameter,  $\mu^1$ . However, a model with negative  $\mu$  and universal gaugino masses [9] predicts a negative SUSY contribution to the muon anomalous magnetic moment,  $(g - 2)_\mu$ , and enlarges the observed discrepancy between theory and experiment. That is why most of the studies that assume universal gaugino mass in the last decade has been devoted to the case of positive  $\mu$  [10, 11]. In such a case Yukawa unification can be realized but there is a price for it. Namely, scalar masses are pushed to the multi-TeV regime so proper REWSB is obtained at the expense of severe fine-tuning. Moreover, these models have serious problems with FCNC constraints [12] because of very large value of  $|\mu A_t|$ , in particular with a lower limit on  $\text{BR}(B_s \rightarrow \mu^+ \mu^-)$  which was recently improved by CMS and LHCb experiments [13].

Last but not least, a value of the gluino mass which is most favourable by Yukawa unification in that class of models is about 350 GeV [14], while the recent ATLAS “b-jet” search [15] excluded gluino masses up to 450 (570) GeV in a model with “ad hoc” splitting of Higgs masses [10] ( $D$ -term splitting of scalar masses [11]). As a result, models with positive  $\mu$  and universal gaugino masses in the part of the parameter space consistent with LHC experiments cannot allow for top-bottom-tau Yukawa unification at a level better than 5%. For a recent review of SO(10) models with the third family Yukawa coupling unification see Ref. [16].

---

<sup>1</sup>We use the sign convention in which the gluino mass parameter  $M_3$  and the gluino mass  $m_{\tilde{g}}$  are positive.

A remedy to problems of SO(10) models discussed above was put forward recently in Ref. [17] where a novel model with negative  $\mu$  was proposed. In that model gaugino masses are assumed to be generated by an  $F$ -term which is a non-singlet of SO(10) transforming as a  $\mathbf{24}$  of  $SU(5) \subset SO(10)$ . Such assumption leads to gaugino masses with the following pattern at the GUT scale:  $M_1 : M_2 : M_3 = -1 : -3 : 2$  [18]. The main phenomenological success of that model is its consistency with all experimental constraints including  $(g - 2)_\mu$  and  $\text{BR}(b \rightarrow s\gamma)$  which are satisfied thanks to a positive sign of the product  $\mu M_2$  [19]. Another advantage of that model is the prediction of a rather light SUSY spectrum which can be tested at the LHC. In particular, the gluino mass is predicted to be in the range of about 500 – 700 or 900 – 1550 GeV. It is not unreasonable to expect that some of the parameter space corresponding to such a light gluino has already been excluded by the LHC. However, LHC experiments interpret their result mainly in the CMSSM and some simplified models and the obtained mass limits for SUSY particles cannot be applied directly to the other models. There are several studies that reinterpret the LHC SUSY searches in terms of the SUSY models other than the CMSSM. The LHC constraints on gauge mediation [20, 21], anomaly mediation [22], phenomenological SUSY models [23, 24], SUSY models with compressed spectra [25] and light third generation models [26, 27, 28, 29, 30] have been studied. The constraints on models with top-bottom-tau Yukawa unification in the context of SUSY  $SU(4)_c \times SU(2)_L \times SU(2)_R$  [31] have also been investigated [32]. In the present paper we study the constraints and implications of recent LHC data on the SO(10) model proposed in Ref. [17]. We focus on three ATLAS analyses of the final states with large missing transverse momentum and no leptons: the “0-lepton” search with  $1.04 \text{ fb}^{-1}$  [33], the “b-jet” search with  $0.83 \text{ fb}^{-1}$  [15] and the “multijet” search with  $1.34 \text{ fb}^{-1}$  of data [34].

The paper is organized as follows. In section 2 we describe in some more detail the SO(10) model proposed in Ref. [17]. In section 3 we summarise the ATLAS searches for squark and gluinos. In section 4 we present our methodology of simulating ATLAS searches and its validation. Interpretation of ATLAS searches in the SO(10) model proposed in Ref. [17] is given in section 5. We conclude in section 6. In the Appendix we give additional information on the validation of our simulation of ATLAS searches.

## 2 Description of the SO(10) model

We start with a brief review of the SO(10) model proposed in Ref. [17]. The first crucial feature of this model is that the Higgs-mixing parameter  $\mu$  is negative. Negative sign of  $\mu$  is phenomenologically preferred because it allows for negative threshold correction to the bottom mass [1, 2, 3] (as required by Yukawa unification) without the need to push up scalar masses to multi-TeV regime. Even though negative  $\mu$  is preferred by Yukawa unification, it leads to discrepancy with the experimental results for  $(g - 2)_\mu$  and  $\text{BR}(b \rightarrow s\gamma)$  if gaugino masses are universal. As explained in detail in Ref. [17], phenomenologically acceptable models require  $\mu M_2 > 0$ . In order to satisfy this condition gaugino masses are assumed to be generated by non-zero  $F$ -term of a 24-dimensional representation of  $SU(5) \subset SO(10)$ . This leads to the

following pattern of gaugino masses at the GUT scale [18]:

$$(M_1, M_2, M_3) = \left(-\frac{1}{2}, -\frac{3}{2}, 1\right) M_{1/2}. \quad (1)$$

It should be stressed that even though non-universalities in gaugino masses are introduced, only one free parameter,  $M_{1/2}$ , governs the gaugino sector.

The soft scalar masses also need to be non-universal to achieve Yukawa unification and light sparticle spectrum<sup>2</sup>. It is assumed that the  $D$ -term of the  $U(1)_V$  ( $SO(10) \supset SU(5) \times U(1)_V$ ) vector superfield acquires a vacuum expectation value at the GUT scale<sup>3</sup>. The scalar masses, then, can be written as

$$\begin{aligned} m_{H_d}^2 &= m_{10}^2 + 2D, \\ m_{H_u}^2 &= m_{10}^2 - 2D, \\ m_{Q,U,E}^2 &= m_{16}^2 + D, \\ m_{D,L}^2 &= m_{16}^2 - 3D. \end{aligned} \quad (2)$$

Such a contribution generically arises in the effective theory below the GUT scale as a consequence of spontaneous breakdown of  $U(1)_V$  at the GUT scale [7]. Finally, it is assumed that soft trilinear couplings have an universal value  $A_0$  at the GUT scale.

It was shown in Ref. [8] that for universal gaugino masses top-bottom-tau Yukawa unification can be realized only if  $D > 0$  and  $m_{10} > m_{16}$ . The same conditions are preferred in the  $SO(10)$  model studied in Ref. [17] where gaugino masses are given in Eq. (1). Moreover, it was noted in Ref. [17] that Yukawa unification consistent with REWSB requires specific correlations between parameters  $D$ ,  $m_{10}$  and  $A_0$ . Provided that these correlations hold, top-bottom-tau Yukawa unification can be realized for a very wide range of  $M_{1/2}$  and  $m_{16}$ . Non-trivial constraints on the model are obtained from  $BR(b \rightarrow s\gamma)$ ,  $(g - 2)_\mu$  and the upper bound on the relic abundance of the lightest neutralinos,  $\Omega_{DM}h^2$ . Given that these observables are consistent with the experimental data, the assumption of Yukawa unification leads to rather definite prediction for the MSSM spectrum. This is mainly due to the tension between  $BR(b \rightarrow s\gamma)$  and  $(g - 2)_\mu$ : the former prefers heavy SUSY spectrum while the latter the light one. On top of that, the WMAP bound [37] on  $\Omega_{DM}h^2$  can be satisfied only in some corners of the parameter space where various mechanisms which enhance annihilation cross-section of the LSP are at work. It was found in Ref. [17] that in the part of the parameter space where Yukawa unification is

---

<sup>2</sup> In Ref. [35] Yukawa-unified solutions with gaugino masses given in Eq. (1) and universal scalar masses were found. However, the price for the universality in the scalar sector is very heavy spectrum of squarks and gluinos inaccessible at the LHC. Moreover, such solutions predict too small SUSY contribution to  $(g - 2)_\mu$  to be consistent with the experimental data. In the present paper we demand that the constraint from  $(g - 2)_\mu$  is satisfied at least at  $2\sigma$  level.

<sup>3</sup> In Ref. [36] a model with  $\mu < 0$  and non-universal gaugino masses given in Eq. (1) was considered in which sfermion masses are assumed to be universal and ‘‘ad hoc’’ Higgs mass splitting is introduced which explicitly breaks  $SO(10)$  gauge symmetry.

consistent simultaneously with  $\text{BR}(b \rightarrow s\gamma)$  and  $(g-2)_\mu$ , the gluino mass is predicted to have any value below about 1550 GeV. However, in the region of the parameter space where gluino mass is below about 500 GeV and between about 700 and 900 GeV there is no efficient LSP annihilation mechanism that could reduce the thermal relic abundance of the neutralinos to acceptable values.

For the gluino mass between about 500 and 700 GeV WMAP bound on  $\Omega_{\text{DM}}h^2$  can be satisfied due to resonant annihilations of the LSP through the  $Z$  boson or the lightest CP-even Higgs exchange. Throughout this paper we will refer to the region of the parameter space with efficient LSP annihilation via  $Z$  or  $h^0$  as the light gluino region. In light of the recent LHC data it is not clear whether model points with such a light gluino are still allowed. In Ref. [33] ATLAS collaboration presented interpretation of the 0-lepton search in the simplified model in which all sparticles except for gluino, degenerate squarks of the first and second generation and massless neutralino are decoupled. In such a model gluino with mass below 700 GeV has been excluded at 95% C.L. for squark masses up to 2 TeV, with the limit increasing to 1075 GeV for equal mass squarks and gluinos. In the light gluino region of the SO(10) model of Ref. [17], the masses of  $\tilde{u}_R$ ,  $\tilde{u}_L$  and  $\tilde{d}_L$  (which are degenerate to large extent) are in the range 1.1-1.6 TeV, while the mass of  $\tilde{d}_R$  (which is always lighter than the other first generation squarks due to the  $D$ -term splitting of soft scalar masses) is between about 900 and 1300 GeV. Applying limits on the gluino and squark masses in the simplified model to that SO(10) model one would exclude the light gluino region. However, limits on the gluino and squarks masses in the simplified model described above should be treated as an useful indication to what extent gluino and squark masses can be constrained with the available LHC data. For realistic models, these limits will be typically weaker. One of the main purposes of the present paper is to check whether the light gluino region of the SO(10) model of Ref. [17] is still allowed by the recent LHC data.

There are at least two reasons why limits from the 0-lepton search on the squark and gluino masses in the SO(10) model of [17] may be substantially weaker than in the simplified model. First, winos and Higgsinos are always lighter than gluino at the EW scale<sup>4</sup>. Therefore, gluino usually decays to chargino or neutralino other than bino-like LSP, unlike in the simplified model where gluino decays to  $q\bar{q}\tilde{\chi}_1^0$  through an off-shell squark. Second, in some part of the parameter space right-handed sbottom is lighter than the gluino. For such model points gluino decays exclusively to  $\tilde{b}_1$  (associated with b-jet) which subsequently decays most of the times to Higgsino-like neutralino or chargino unless these decays are kinematically inaccessible. Longer gluino decay chain results on average in smaller  $p_T$  of individual jets and such events are less likely to pass the selection cuts.

In the second region with the gluino mass between about 900 and 1550 GeV three mechanisms enhancing LSP annihilations may be at work: t-channel exchange of the right-handed sbottom, resonant annihilation through CP-odd Higgs,  $A^0$ , and coannihilations with the stau. The first aforementioned mechanism requires sbottom to be lighter than about 200 GeV.

---

<sup>4</sup>  $M_3 \sim -2M_2 \sim -12M_1$  at the EW scale.

Yukawa-unified solutions with such a light sbottom has been found in the numerical scan performed in Ref. [17] but only in the part of the parameter space where the LSP mass is below 100 GeV. Such solutions are excluded at 95% C.L. by D0 search at the Tevatron [38]. Yukawa-unified solutions, in which the LSP annihilation via  $A^0$  exchange dominates the total annihilation cross-section, were ruled out very recently by the LHC direct  $A^0 \rightarrow \tau\tau$  searches. This follows from the fact that the LSP annihilation via  $A^0$  exchange in the SO(10) model of Ref. [17] can be large enough only when  $m_{A^0} \lesssim 400$  GeV and  $\tan\beta$  between 45 and 50, while the ATLAS [39] and CMS [40] analyses excluded  $m_{A^0}$  below 400 (450) GeV for  $\tan\beta \approx 45$  (50) at 95% C.L.. The limits on the  $(m_{A^0}, \tan\beta)$  plane do not depend significantly on the other MSSM parameters [41], and these limits are also applicable to that SO(10) model in a rather good approximation.

The regions of the parameter space where the WMAP bound is satisfied due to stau coannihilation are not constrained by any experiment so far. Values of gluino mass found in stau-coannihilation region are between about 1000 and 1550 GeV, the masses of  $\tilde{u}_L$  and  $\tilde{d}_L$  are in the range 1.3-1.8 TeV, while  $\tilde{u}_R$  ( $\tilde{d}_R$ ) are lighter by about 100 (300) GeV than left-handed squarks. In contrast to the light gluino mass region, in the stau-coannihilation region gluino is always heavier than all third generation squarks and often heavier than  $\tilde{d}_R$ . Most importantly,  $\tilde{b}_1$  is always lighter than the gluino by at least 500 GeV which imply that sbottom production is comparable or even more significant than gluino and first generation squarks production. Notice that spectra corresponding to the stau-coannihilation region are too heavy to be excluded even if one applies the limits found in the simplified model with gluino, LSP and only first generation squarks (based on the 0-lepton search) and the simplified model with gluino, LSP and lighter sbottom (based on the b-jet search) which typically overestimate the true exclusion limits. Nevertheless, we include this region in our analysis to confirm this expectation.

There is also a part of the parameter space where both the  $A^0$  exchange and stau-coannihilation contribute to the LSP annihilation cross-section at similar rate and the WMAP bound is satisfied. In this region, the required  $A^0$  mass has not been excluded by the current LHC searches. However, we should comment that such solutions require  $m_{A^0}$  to be smaller than about 480 GeV, and those solutions may be excluded when the whole LHC data accumulated in 2011 are analysed. Gluino and squark spectra corresponding to such solutions are similar to those for the stau-coannihilation region.

Finally, we should also comment on the fact that the only Yukawa-unified solutions corresponding to the gluino mass in the range 900 – 1000 GeV are those with a very light sbottom or  $m_{A^0} \lesssim 400$ . As we pointed out above, the former are excluded by the Tevatron while the latter are excluded by the LHC. This is an interesting example of a case in which parameter  $M_{1/2}$  and thus the gluino mass can be constrained not because of excessive production of gluinos in  $pp$  collisions but as a consequence of some correlations between MSSM parameters in a specific subclass of MSSM models.

Signal Region	$\geq 2$ jets	$\geq 3$ jets	$\geq 4$ jets low	$\geq 4$ jets high	High mass
$E_T^{\text{miss}}$	$> 130$	$> 130$	$> 130$	$> 130$	$> 130$
Leading jet $p_T$	$> 130$	$> 130$	$> 130$	$> 130$	$> 130$
Second jet $p_T$	$> 40$	$> 40$	$> 40$	$> 40$	$> 80$
Third jet $p_T$	-	$> 40$	$> 40$	$> 40$	$> 80$
Fourth jet $p_T$	-	-	$> 40$	$> 40$	$> 80$
$\Delta\phi_{\text{min}}$	$> 0.4$	$> 0.4$	$> 0.4$	$> 0.4$	$> 0.4$
$E_T^{\text{miss}}/m_{\text{eff}}$	$> 0.3$	$> 0.25$	$> 0.25$	$> 0.25$	$> 0.2$
$m_{\text{eff}}$	$> 1000$	$> 1000$	$> 500$	$> 1000$	$> 1100$
SM Background	$62.4\pm 4.4\pm 9.3$	$54.9\pm 3.9\pm 7.1$	$1015\pm 41\pm 144$	$33.9\pm 2.9\pm 6.2$	$13.1\pm 1.9\pm 2.5$
Data	58	59	1118	40	18

Table 1: The cuts used to define signal regions of the ATLAS 0-lepton analysis [33]. All dimensionful quantities are given in GeV.  $\Delta\phi_{\text{min}}$  is the minimum azimuthal angle between  $\vec{p}_T^{\text{miss}}$  and  $\vec{p}_T$  of the three leading jets. The number of events observed by ATLAS in each signal region, as well as the expected Standard Model background are also displayed. The first uncertainty represents the statistical uncertainty, while the second is the systematic one.

### 3 ATLAS searches for squarks and gluinos

In order to investigate the LHC constraints on the SO(10) model we focus in this paper on ATLAS searches for SUSY, although one can expect that the limits from CMS searches are comparable. The 0-lepton search performed by ATLAS [33] with  $1.04 \text{ fb}^{-1}$  of data defines five signal regions with at least two, three or four jets. The main kinematic variables used in that analysis is the effective mass,  $m_{\text{eff}}$ , and the magnitude of the missing transverse momentum  $E_T^{\text{miss}} \equiv |\vec{p}_T^{\text{miss}}|$ .  $m_{\text{eff}}$  is defined as the sum of  $E_T^{\text{miss}}$  and the magnitudes of the transverse momentum,  $p_T \equiv |\vec{p}_T|$ , of two, three or four leading jet for the signal region with at least two, three or four jets, respectively. In the ‘‘high mass’’ signal region, however,  $m_{\text{eff}}$  is defined as the sum of  $E_T^{\text{miss}}$  and  $p_T$  of all jets with  $p_T > 40$  GeV. All signal regions require high  $p_T$  jets and large  $E_T^{\text{miss}}$ . The cuts applied in each signal region of the 0-lepton search are summarized in Table 1.

In the SO(10) model of Ref. [17], the right-handed sbottom is the lightest among the squarks. In some part of the parameter space sbottom is even lighter than the gluino. Therefore, one may expect that sbottoms are significantly produced at the LHC, either directly from proton-proton collisions or indirectly from gluino decays. In consequence, a lot of b-jets are expected in typical final state. That is why we use also the ATLAS b-jets 0-lepton analysis [15] with  $0.83 \text{ fb}^{-1}$  of data to set constraints on that SO(10) model. In that analysis four signal regions have been defined with the requirement of three or more jets and at least one or two b-jets, depending on the signal regions. In the ATLAS b-jet analysis the same kinematic variables as in the 0-lepton search are used. Since one of the main targets of the b-jet 0-lepton analysis is constraining

Signal Region	3JA	3JB	3JC	3JD
$E_T^{\text{miss}}$	$> 130$	$> 130$	$> 130$	$> 130$
Leading jet $p_T$	$> 130$	$> 130$	$> 130$	$> 130$
Second jet $p_T$	$> 50$	$> 50$	$> 50$	$> 50$
Third jet $p_T$	$> 50$	$> 50$	$> 50$	$> 50$
Number of b-jets	$\geq 1$	$\geq 1$	$\geq 2$	$\geq 2$
$\Delta\phi_{\text{min}}$	$> 0.4$	$> 0.4$	$> 0.4$	$> 0.4$
$E_T^{\text{miss}}/m_{\text{eff}}$	$> 0.25$	$> 0.25$	$> 0.25$	$> 0.25$
$m_{\text{eff}}$	$> 500$	$> 700$	$> 500$	$> 700$
SM Background	$356^{+103}_{-92}$	$70^{+24}_{-22}$	$79^{+28}_{-25}$	$13^{+5.6}_{-5.2}$
Data	361	63	76	12

Table 2: The cuts used to define signal regions of the ATLAS b-jets 0-lepton analysis [15].

models which predict light sbottoms, the cuts on  $m_{\text{eff}}$  are weaker than in the 0-lepton search. The cuts defining four signal regions of the b-jet 0-lepton search are summarized in Table 2.

Another analysis which may be sensitive to the SO(10) model was released most recently and focuses on search for new phenomena with large jet multiplicities and missing transverse momentum [34] using  $1.34 \text{ fb}^{-1}$  of data. Throughout this paper we will refer to that analysis as the multijets analysis. In that analysis events with leptons in the final state are discarded. Four different signal regions have been defined with the minimum number of jets varying between six and eight. For such a large number of jets large trigger inefficiencies may occur. In order to maintain acceptable trigger efficiency a separation  $\Delta R_{jj} > 0.6$  between all jets with  $p_T$  above the threshold for a given signal region is required. Large missing transverse energy is required due to the cut on  $E_T^{\text{miss}}/\sqrt{H_T}$  where  $H_T$  is the scalar sum of the transverse momenta of all jets with  $p_T > 40 \text{ GeV}$  and  $|\eta| < 2.8$ . The cuts applied in each signal region of the multijets search are detailed in Table 3.

The primary target of the multijets analysis is to provide increased sensitivity to models with sequential decays to many strongly interacting particles. It therefore fits very well for the purpose of constraining the SO(10) model. The multijets analysis has already been proved to be useful in the context of CMSSM for which constraints in the region where  $m_{1/2} \ll m_0$  from multijets analysis are comparable (or even better if  $m_0$  is between about 1 and 1.5 TeV) to the ones from the 0-lepton search [34].

For each signal region  $i$ , the ATLAS papers provide the information on the observed number of events  $n_o^{(i)}$ , expected number of Standard Model background events  $n_b^{(i)}$  together with its error  $\sigma_b^{(i)}$ . These numbers are given in Tables 1, 2, 3. The agreement between  $n_o^{(i)}$  and  $n_b^{(i)}$  can place constraints on SUSY models which predict the expected signal events  $n_s^{(i)}$  with its error  $\sigma_s^{(i)}$ . In the next section we describe our procedure of computing  $n_s^{(i)}$  and  $\sigma_s^{(i)}$  and validate it against the ATLAS exclusion plots for the CMSSM (in the case of the 0-lepton [33] and the multijets [34] analyses) and the simplified model with gluino, sbottom and lightest neutralino (in the



Signal Region	7j55	8j55	6j80	7j80
Jet $p_T$	$> 55$ GeV		$> 80$ GeV	
$\Delta R_{jj}$	$> 0.6$ for any pair of jets			
Number of jets	$\geq 7$	$\geq 8$	$\geq 6$	$\geq 7$
$E_T^{\text{miss}}/\sqrt{H_T}$	$> 3.5$ GeV $^{1/2}$			
SM Background	$39 \pm 9$	$2.3^{+4.4}_{-0.7}$	$26 \pm 6$	$1.3^{+0.9}_{-0.4}$
Data	45	4	26	3

Table 3: The cuts used to define signal regions of the ATLAS multijets analysis [34].

case of the b-jet analysis [15]).

## 4 Methodology and its validation

Let us now discuss our methodology of simulating the ATLAS searches. We use various publicly available codes. First, we compute SUSY spectra with SOFTSUSY [42] whose outputs are passed to SUSYHIT [43] which calculates branching ratios for all SUSY particles. We simulate SUSY events using Herwig++ [44] where the effects of parton shower, hadronization and underlying events are taken into account. 10000 events are generated for each model point. In the simulation we include only production channels with at least one squark or gluino. We do not simulate direct pair productions of neutralinos, charginos or sleptons since they are either negligible or  $p_T$  of jets and effective mass,  $m_{\text{eff}}$ , corresponding to such events are too small to pass the selection cuts. Detector simulation is done using Delphes [45] with the ATLAS detector card modified according to the ATLAS analyses, where in particular jets are defined using anti- $k_T$  algorithm with  $\Delta R = 0.4$  and b-jet tagging efficiency is set to 50%. Finally, the total SUSY production cross-section,  $\sigma_{\text{NLO}}$ , is calculated at next-to-leading order with PROSPINO [46].

In order to work out the expected number of SUSY events in signal region  $i$ ,  $n_s^{(i)}$ , we apply the cuts detailed in Tables 1, 2, 3 to find their efficiency  $\epsilon$  (i.e. the ratio of the number of events that survived the cuts to the total number of generated events).  $n_s^{(i)}$  is given by  $\sigma_{\text{NLO}} \times \epsilon^{(i)} \times \mathcal{L}^{(i)} \times A^{(i)}$ , where  $A^{(i)}$  is a correction factor which accounts for the impact of additional data cleaning due to electronics failure in one of the calorimeters in the ATLAS detector during some period of data-taking. We take  $A = 0.9$  for the b-jet analysis and  $A = 0.95$  for the 0-lepton and the multijets analyses.

In order to estimate the exclusion limits we mimic the ATLAS analyses to the extent that is allowed by the limited amount of information provided in the ATLAS publications on those analyses. In particular, CLs method [47] is used which employs variable  $CLs$  defined by:

$$CLs \equiv \frac{p_{s+b}}{1 - p_b}, \quad (3)$$

to set the exclusion limits on a model at  $(1 - CL_s) \times 100\%$  confidence level, which means a model is excluded at 95% C.L. if  $CL_s < 0.05$ . In the above definition  $p_{s+b}$  is the p-value of the background plus signal hypothesis while  $p_b$  is the p-value of the background only hypothesis. Given the information  $\vec{\Sigma}^{(i)} = (n_s^{(i)}, n_b^{(i)}, \sigma_s^{(i)}, \sigma_b^{(i)})$  for each signal region  $i$ , p-values are computed in the following way [48]:

$$p_{s+b}(n_o^{(i)}) = \sum_{n=0}^{n_o^{(i)}} P(n|\vec{\Sigma}^{(i)}), \quad p_b(n_o^{(i)}) = \sum_{n=n_o^{(i)}}^{\infty} P(n|\vec{\Sigma}^{(i)}), \quad (4)$$

where  $P(n|\vec{\Sigma}^{(i)})$  is the probability of observing  $n$  events in the signal region  $i$  which is governed by Poisson distribution with the expectation value for the observed events:

$$\lambda^{(i)}(\vec{\Sigma}^{(i)}, \delta_b, \delta_s) = n_b^{(i)}(1 + \delta_b \sigma_b^{(i)}) + n_s^{(i)}(1 + \delta_s \sigma_s^{(i)}), \quad (5)$$

where the impact of the uncertainties on the expected number of events is accounted for by the nuisance parameters  $\delta_b$  and  $\delta_s$ . We have neglected the error on the luminosity since it is negligible as compared to the errors we included. Assuming that the nuisance parameters have Gaussian probability distribution function, the probability of observing  $n$  events is given by:

$$P(n|\vec{\Sigma}^{(i)}) = \int_{-1/\sigma_s^{(i)}}^{\infty} d\delta_s \int_{-1/\sigma_b^{(i)}}^{\infty} d\delta_b \frac{e^{-\lambda^{(i)}} (\lambda^{(i)})^n}{n!} e^{-\frac{1}{2}(\delta_s^2 + \delta_b^2)}. \quad (6)$$

The lower limit of the integration is restricted to keep the number of signal and background events independently non-negative.

The ATLAS papers provide the error on the signal cross-section. It is estimated by varying the renormalization and factorization scales in PROSPINO between half and twice their default value and by considering the PDF uncertainties provided by CTEQ [49]. The resulting uncertainties on signal cross-section vary somewhat from point to point in parameter space but it is reasonable to assume that the error on cross-section for each production channel is constant across the parameter space. In our analysis we assign uncertainties of 10%, 20%, 30%, 35% for  $\tilde{q}\tilde{q}$  and  $\tilde{q}\tilde{q}^*$ ,  $\tilde{q}\tilde{g}$ ,  $\tilde{g}\tilde{g}$ ,  $\tilde{t}\tilde{t}^*$  and  $\tilde{b}\tilde{b}^*$  productions, respectively.

The ATLAS papers do not provide, however, details on other systematic uncertainties on the signal such as jet energy scale uncertainty or b-tagging uncertainty. We model these uncertainties by taking a constant value  $\sigma_{s'}^{(i)}$  for signal region  $i$ . Our estimation of the total systematic uncertainty on the signal is then given by  $\sigma_s^{(i)} = \sqrt{\sigma_{\text{cross}}^2 + \sigma_{s'}^{(i)2}}$ . In order to determine  $\sigma_{s'}^{(i)}$  we adjust it manually in such a way that our 95% C.L. exclusion contours match the official ones presented in the ATLAS publications.

We find that  $\sigma_{s'}^{(3JD)} = 0.6$  reproduces the official ATLAS exclusion contours from b-jet analysis [15] in the simplified model containing only gluino, sbottom and the lightest neutralino with mass 60 GeV reasonably well<sup>5</sup>, as seen from Figure 1. In the official ATLAS plot exclusion contours are restricted to the region of parameter space in which gluino mass is larger than the

<sup>5</sup>We do not include in our analysis 3JA, 3JB and 3JC signal regions of the b-jet search because exclusion

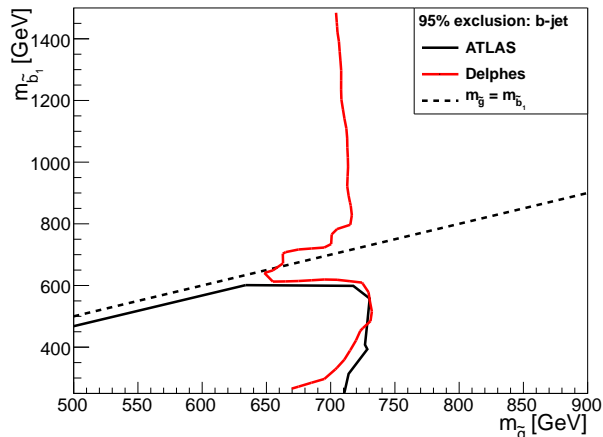


Figure 1: Comparison of our 95% exclusion contours with those of ATLAS in a simplified model in which only gluino, lighter sbottom and the LSP with mass of 60 GeV are in low energy spectrum, while all other sparticles are decoupled. In contrast to ATLAS exclusion contours, ours cover also some region of parameter space where  $m_{\tilde{g}} < m_{\tilde{b}_1} + m_b$ .

sum of sbottom and bottom masses. In Figure 1 we present extended version of that plot to the region of parameter space where  $m_{\tilde{g}} < m_{\tilde{b}_1} + m_b$  and gluino decays through off-shell sbottom to  $b\bar{b}\tilde{\chi}_1^0$ .

We also find that  $\sigma_{s'}^{(2j)} = \sigma_{s'}^{(3j)} = \sigma_{s'}^{(4j\text{high})} = 0.3$  and  $\sigma_{s'}^{(\text{hm})} = \sigma_{s'}^{(3j)} = \sigma_{s'}^{(4j\text{low})} = 0.1$  give a rather good approximation of the ATLAS exclusion contours for the 0-lepton search, as seen from Figure A.1 in the Appendix. For the multijet analysis we find the best fit for  $\sigma_{s'}^{(7j55)} = \sigma_{s'}^{(8j55)} = \sigma_{s'}^{(6j80)} = \sigma_{s'}^{(7j80)} = 0.1$ , as seen from Figure A.2 in the Appendix.

## 5 ATLAS constraints on the SO(10) model

We are now ready to present resulting constraints on the SO(10) model from our simulation of the ATLAS analyses. We analysed 977 points (out of which 490 are in the light gluino region) satisfying top-bottom-tau Yukawa unification at the level of 10% or better found in a numerical scan performed in Ref. [17]. All of these points satisfy the following experimental constraints

---

plots for individual signal regions has not been made publicly available so it was not possible to validate our simulation of these signal regions. We do not expect that inclusion of these signal regions would change our conclusions significantly since 3JD signal region is the most constraining one in the vast majority of the parameter space [15].

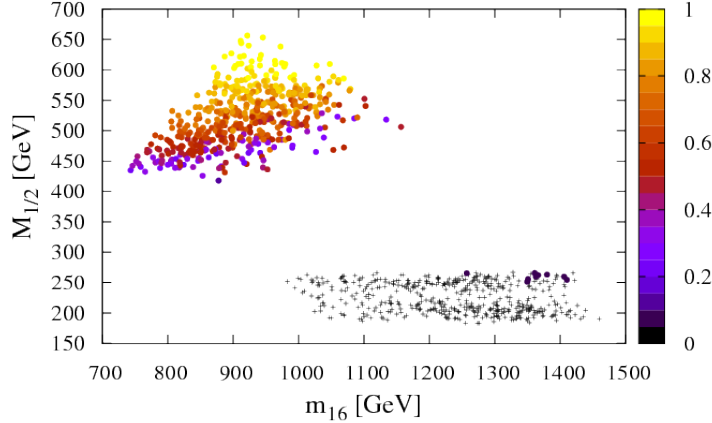


Figure 2: Distribution of the  $CLs$  value in the  $m_{16} - M_{1/2}$  plane based on the combination of the 0-lepton, the b-jet and the multijets searches. For each point in the plot, the signal region providing the smallest value of  $CLs$  is chosen. Black crosses correspond to points excluded at 95% C.L..

(which were computed with appropriate routines in MicrOmegas [50]):

$$12.7 \cdot 10^{-10} < \delta a_{\mu}^{SUSY} < 44.7 \cdot 10^{-10} \quad (2\sigma) \quad [51]$$

$$2.89 \cdot 10^{-4} < \text{BR}(b \rightarrow s\gamma) < 4.21 \cdot 10^{-4} \quad (2\sigma) \quad [52]$$

$$\text{BR}(B_s \rightarrow \mu^+ \mu^-) < 1.08 \cdot 10^{-8} \quad [13]$$

$$\Omega_{\text{DM}} h^2 < 0.1288 \quad (3\sigma) \quad [37]$$

$$m_{h^0} > 111.4 \text{ GeV} \quad [53]$$

Notice that we have included the recent constraint on  $\text{BR}(B_s \rightarrow \mu^+ \mu^-)$  from combined analysis of CMS and LHCb [13]. However, this observable is much less constraining than the lower limit on  $m_{A^0}$  which we set in our analysis at 400 GeV independently of  $\tan \beta$  (which varies between about 45 and 50 in the region of parameter that might be affected by present constraint on  $m_{A^0}$ ). We use slightly relaxed bound on  $m_{A^0}$  due to its (small) model dependence and theoretical uncertainty in the prediction of  $m_{A^0}$ . The mass limits on SUSY particles from LEP and Tevatron including limit on the sbottom mass discussed in section 2 are also taken into account. Due to the fact that the uncertainty in the prediction of the lightest Higgs boson mass is about 3 GeV [54] slightly relaxed LEP2 bound [53] is used. Even though, we require model points to satisfy only the upper WMAP bound, many of them satisfy also the lower WMAP bound on dark matter relic density.

The main result of our analysis is that 481 out of 490 points in the light gluino region are excluded at 95% C.L.. On the other hand, none of the points are excluded in the stau-coannihilation region. This can be seen from Figure 2 where the distribution of the  $CLs$  value

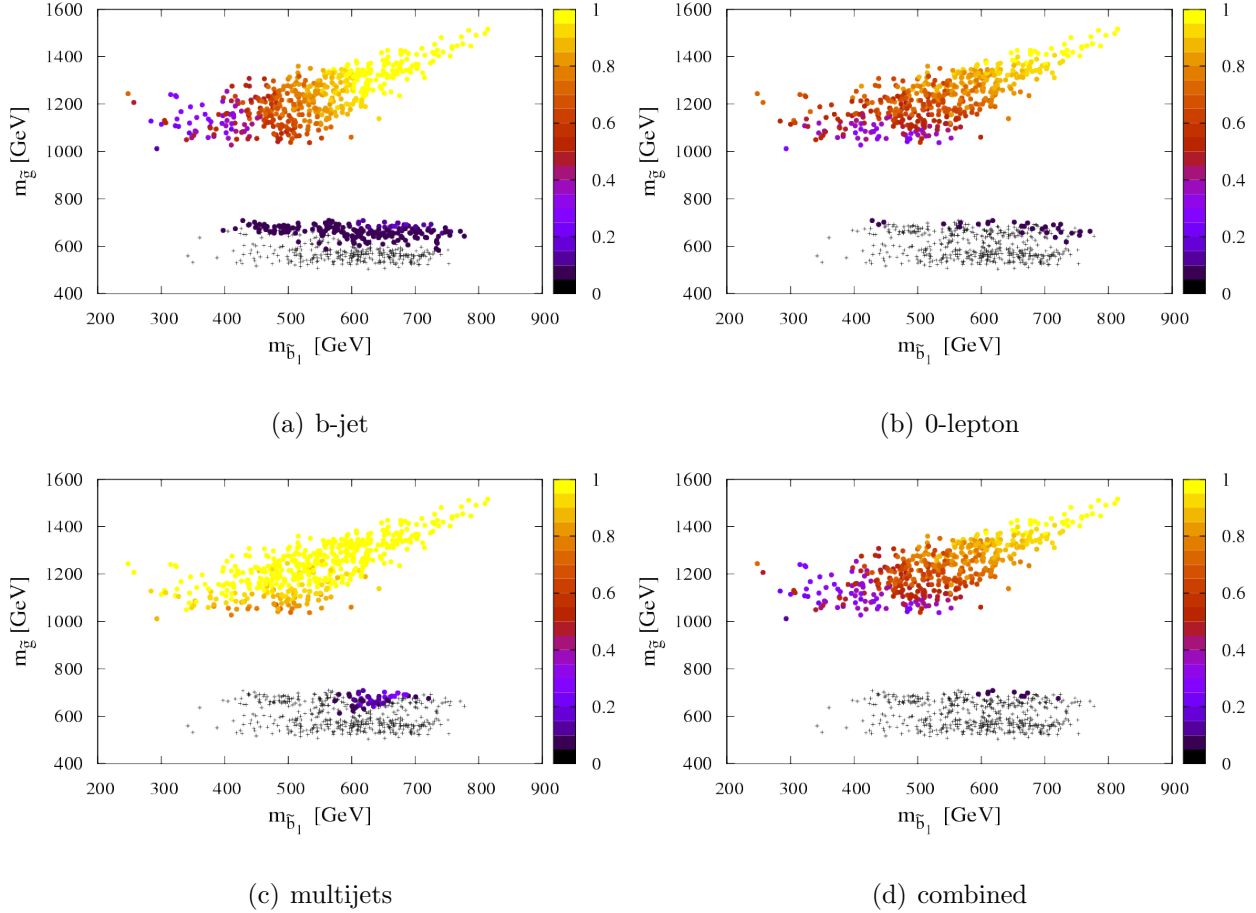


Figure 3: Distribution of the  $CLs$  value in the  $m_{\tilde{b}_1} - m_{\tilde{g}}$  plane based on: (a) the b-jet search only, (b) the 0-lepton search only, (c) the multijets search only, (d) the combination of all searches. Black crosses correspond to points excluded at 95% C.L..

in the  $m_{16} - M_{1/2}$  plane based on the combination of all searches is presented. For each point in this plot, the signal region providing the smallest  $CLs$  value is chosen. The model points depicted by crosses are excluded at 95% C.L..

In Figures 3 and 4, distributions of the  $CLs$  values based on individual searches and their combination are shown in the  $m_{\tilde{d}_R} - m_{\tilde{g}}$  and  $m_{\tilde{b}_1} - m_{\tilde{g}}$  planes, respectively. The first thing to note from these Figures is that the 0-lepton and the multijets analyses provide the most stringent constraints on the light gluino region but the b-jet search is only slightly less constraining ruling out by itself about 60% of points in this region. In Table 4 fractions of excluded points in the light gluino region by individual signal regions are shown. In the 0-lepton analysis essentially only “high mass” region is relevant, while in the multijets analysis all signal regions are relevant and complement each other. We should also emphasise the complementarity between the 0-lepton and the multijets searches. While, individually these searches constrain gluino mass to

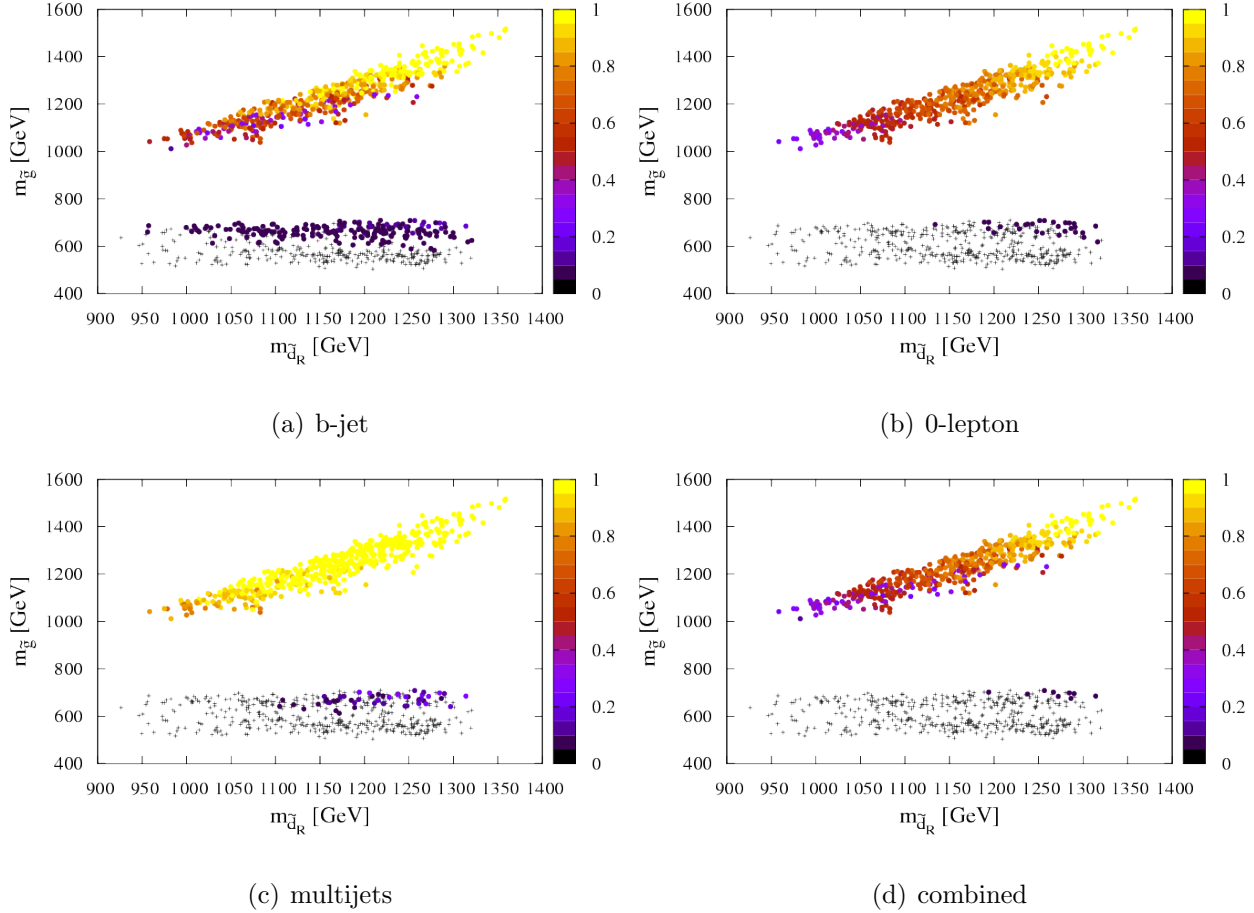


Figure 4: The same as in Figure 3 but in the  $m_{\tilde{d}_R} - m_{\tilde{g}}$  plane.

values above about 620 and 610 GeV, respectively, their combination excludes all points with the gluino mass below about 675 GeV. The multijets analysis is less sensitive to a part of the parameter space where  $m_{\tilde{g}} > m_{\tilde{b}_1}$  and the mass splitting between gluino and sbottom is small. In such a case gluino to sbottom decays produce rather soft jets. This implies that passing the cuts with large jets multiplicities in such a case becomes less likely<sup>6</sup>. Appearance of soft jets in the final state affects also efficiency of “high mass” selection of the 0-lepton search but in a milder way, so some of the points (but not all) with small mass splitting between sbottom and gluino which are not excluded by the multijets analysis are excluded by the 0-lepton search. As a result, all points in the light gluino region which are still allowed are characterized by rather small mass splitting between gluino and sbottom - below about 100 GeV, as can be seen from

<sup>6</sup> Note that our setup of event simulation does not take account of NLO matrix element correction with extra hard jets associated with sparticle production. Including that contribution may slightly increase the efficiency for the events with soft jets from SUSY cascade decays. In this sense, our exclusion provides a conservative limit.

b-jet	0-lepton						multijets					
3JD	2j	3j	4j low	4j high	hm	comb	7j55	8j55	6j80	7j80	comb	comb
59.2	0	8.6	0	24.5	94.1	94.1	74.3	85.9	87.3	44.1	90	98.2

Table 4: Percentage of excluded points at 95% C.L. in the light gluino region by individual signal regions. “comb” in the 0-lepton (multijets) column correspond to a combination of all signal regions within the 0-lepton (multijets) search, while “comb” in the last column correspond to the combination of all three ATLAS searches.

Figure 3. Another feature of the points not excluded by any ATLAS search is rather heavy  $\tilde{d}_R$ . The lower bound on its mass in the light gluino region is found to be about 1.2 TeV, as clearly seen from Figure 4.

It is also interesting to note that all model points in the light gluino region would be excluded if the ATLAS had not observed some small excess over the background (about  $1\sigma$ ) in the high mass signal region of the 0-lepton analysis (see the last column in Table 1). Therefore, if the excess observed by ATLAS is just an upward fluctuation of the background, and not manifestation of SUSY events, the light gluino region will be excluded very soon.

Even though, all of the points in the stau-coannihilation region are consistent with the present LHC data, one can draw some interesting conclusions from our analysis for this case too. First of all, the values of  $CLs$  provided by the b-jet and the 0-lepton search are much smaller than those of the multijets search. This is because in stau-coannihilation region the mass of lighter sbottom is typically comparable to Higgsino mass<sup>7</sup> and  $\tilde{b}_1 \rightarrow \tilde{\chi}_1^- t$  decay channel is closed. Sbottom decaying through this channel may produce even five jets if  $\tilde{\chi}_1^-$  decays subsequently to  $\tilde{\chi}_1^0 W$  so this channel being closed results in big loss of cuts efficiency in the multijets analysis. Even if  $\tilde{b}_1 \rightarrow \tilde{\chi}_1^- t$  decay channel is open, as is the case for a small number of points in the stau-coannihilation region,  $\tilde{\chi}_1^-$  decays usually to  $\tilde{\nu}_\tau \tau$  or  $\tilde{\tau}_1 \nu_\tau$  rather than to  $\tilde{\chi}_1^0 W$  which results in leptons or at least smaller number of hard jets in the final state making implausible to pass the selection cuts used in the multijets analysis. Moreover, efficiency of cuts used in the multijets analysis is reduced also by the fact that  $\tilde{d}_R$  usually decays directly to the LSP producing only single jet.

The 0-lepton and the b-jet search set complementary constraints on the stau-coannihilation region. The b-jet search is the most sensitive (i.e. provides the smallest  $CLs$  value) to model points with very light sbottom when the total SUSY cross-section is dominated by sbottom production<sup>8</sup> while the 0-lepton search constrains the most models with light  $\tilde{d}_R$ , as seen from

<sup>7</sup> This is related to the fact that a requirement of bottom-tau Yukawa unification positively correlates  $|\mu|$  with the gluino mass while sbottom is light due to large negative contributions to its mass from  $D$ -term and renormalization group effects of large positive  $A_0$  required for consistency with  $b \rightarrow s\gamma$  constraint (see detailed discussion in Ref. [17]).

<sup>8</sup> During completion of this work new ATLAS analysis was released [55] in which limits on the  $m_{\tilde{b}_1} - m_{\tilde{\chi}_1^0}$  plane were found that surpass those from D0. In that analysis 2 b-jets are required in the final state and cuts are optimized in order to maximize sensitivity for models with light sbottom. That ATLAS search excludes model

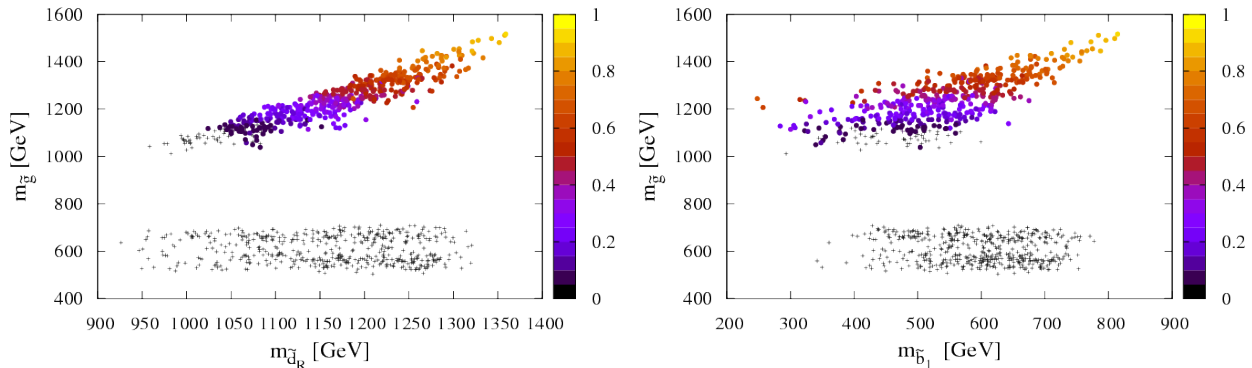


Figure 5: Distribution of expected  $CLs$  value based on the 0-lepton search with  $10 \text{ fb}^{-1}$  of an integrated luminosity.

Figures 3 and 4.

We also estimate prospects for constraining stau-coannihilation region of the SO(10) model with  $10 \text{ fb}^{-1}$  of an integrated luminosity. The multijets search will not have enough sensitivity to exclude any points from this region, as expected from the above discussion. We found that the best prospects for constraining stau-coannihilation region have the 0-lepton search. It can be seen from Figure 5 that the 0-lepton search can probe gluino masses in the stau-coannihilation region up to 1.1 TeV if right-handed down squark is lighter than 1 TeV. In our estimation of expected exclusions with  $10 \text{ fb}^{-1}$  we rescale the statistical errors with the luminosity but keep relative systematic error constant. This is certainly a conservative assumption so the reach of the 0-lepton search may be even better. With this conservative assumption, the b-jet search will not be able to probe the stau-coannihilation region. However, if systematic uncertainties on the background will be reduced significantly, for example due to data driven-methods of systematic error estimation, and/or cuts will be optimized according to larger amount of data, the b-jet search may be complementary to the 0-lepton search, especially in the part of the parameter space with light sbottom.

## 6 Summary and conclusions

We have investigated LHC constraints on the recently proposed SUSY SO(10) GUT model [17] predicting top-bottom-tau Yukawa unification which invokes non-universal gaugino masses arising from SO(10) non-singlet  $F$ -term transforming as  $\mathbf{24}$  of  $SU(5) \subset SO(10)$ ,  $D$ -term splitting of scalar masses and negative sign of  $\mu$ . That model is able to satisfy all experimental constraints including  $(g-2)_\mu$ ,  $b \rightarrow s\gamma$  and predict correct thermal relic abundance of neutralinos. In the

---

points in the stau-coannihilation region with sbottom mass below about 350 GeV if  $\text{BR}(\tilde{b}_1 \rightarrow \tilde{\chi}_1^0 b) = 100\%$  (which is usually the case in this part of the parameter space).



region of parameter space of that SO(10) model where all phenomenological constraints are fulfilled, relatively light MSSM spectrum is predicted making good prospects for its discovery at the LHC. We found that this part of the SO(10) model parameter space tightened considerably due to the recent results of the LHC experiments which have not found any sign of SUSY so far.

The phenomenologically viable parameter space of this model can be classified into three regions in terms of the dominant LSP annihilation process: the light gluino region (the dominant process is  $Z$  boson or light CP-even Higgs exchange), the light  $A^0$  region (the dominant process is CP-odd Higgs exchange) and the stau-coannihilation region (the dominant process is stau-coannihilation.). We have argued that the light  $A^0$  region have already been excluded by the recent  $A \rightarrow \tau\tau$  search at the LHC and we have investigated the impact of the recent direct SUSY searches on the light gluino and stau-coannihilation regions in the SO(10) model.

Since the constraints on gluino and squark masses obtained in the simplified model, where only massless neutralino, gluino and the first/second generation of squarks are assumed in a low energy SUSY spectrum, cannot be directly applied to the other models, we performed dedicated analysis to assess the impact of the recent direct SUSY searches on the SO(10) model. We focused on three ATLAS analyses: the 0-lepton search with  $1.04 \text{ fb}^{-1}$  [33], the b-jet search with  $0.83 \text{ fb}^{-1}$  [15] and the multijet search with  $1.34 \text{ fb}^{-1}$  [34] of data. We found the 95% C.L. lower limit of 675 GeV for the gluino mass, substantially weaker than the one obtained in the simplified model. This implies that the light gluino region is excluded except for the corner of the parameter space where the gluino mass is between 675 GeV and 700 GeV and the right-handed down squark mass is above 1.2 TeV. We, however, stress that the light gluino region would be completely excluded in the absence of the slight excess of events observed in “high mass” signal region of the ATLAS 0-lepton search. Therefore, this region will be excluded very soon unless the observed excess is not just an upward fluctuation of the background.

We also found that the stau-coannihilation region remained unconstrained by the present searches. We have further estimated the expected exclusion limit on this region assuming the same analyses but with  $10 \text{ fb}^{-1}$  of the integrated luminosity at the 7 TeV LHC. The 95% C.L. lower limit on the gluino mass from the 0-lepton search was then found at 1.1 TeV if the right-handed down squark is not heavier than about 1 TeV. The b-jet search may also contribute to the constraints of the stau-coannihilation region, especially in the part of parameter space with light sbottom, if the systematic error in that search is reduced and/or the selection cuts are optimised.

In conclusion, the SO(10) model of Ref. [17] is still consistent with all available direct and indirect constraints with good prospects for testing it at the LHC in the near future. This should be contrasted with Yukawa-unified SO(10) models with universal gaugino masses of which the most favourable part of the parameter space has already been excluded by the LHC experiments. Thus, we believe that the model we studied in the present paper is the best motivated and the most promising SO(10) GUT model which predicts top-bottom-tau Yukawa unification so it is certainly worth further detailed investigation, both, on the theoretical and the experimental side.

# Acknowledgments

This work has been partially supported by STFC. We would like to thank A. Barr and the Cambridge SUSY Working group, particularly B. C. Allanach, B. Gripaios and C. Lester, for helpful discussions. MB would also like to thank M. Olechowski and S. Pokorski for inspiring discussions.

## A Validation of our simulation

In this appendix we present the validation of our simulation of the ATLAS 0-lepton and multijets searches. For each of the signal region in those searches we determine 95% C.L. exclusion region in the  $\tan\beta = 10$ ,  $A_0 = 0$ ,  $\mu > 0$  slice of the CMSSM and compare to the corresponding exclusion region obtained by ATLAS. Such comparisons are shown in Figures A.1 and A.2 for the 0-lepton search and the multijets search, respectively. It can be seen that, for each signal region, our estimation of exclusion contours is similar to the ATLAS one so we conclude that our approximation is reasonable.

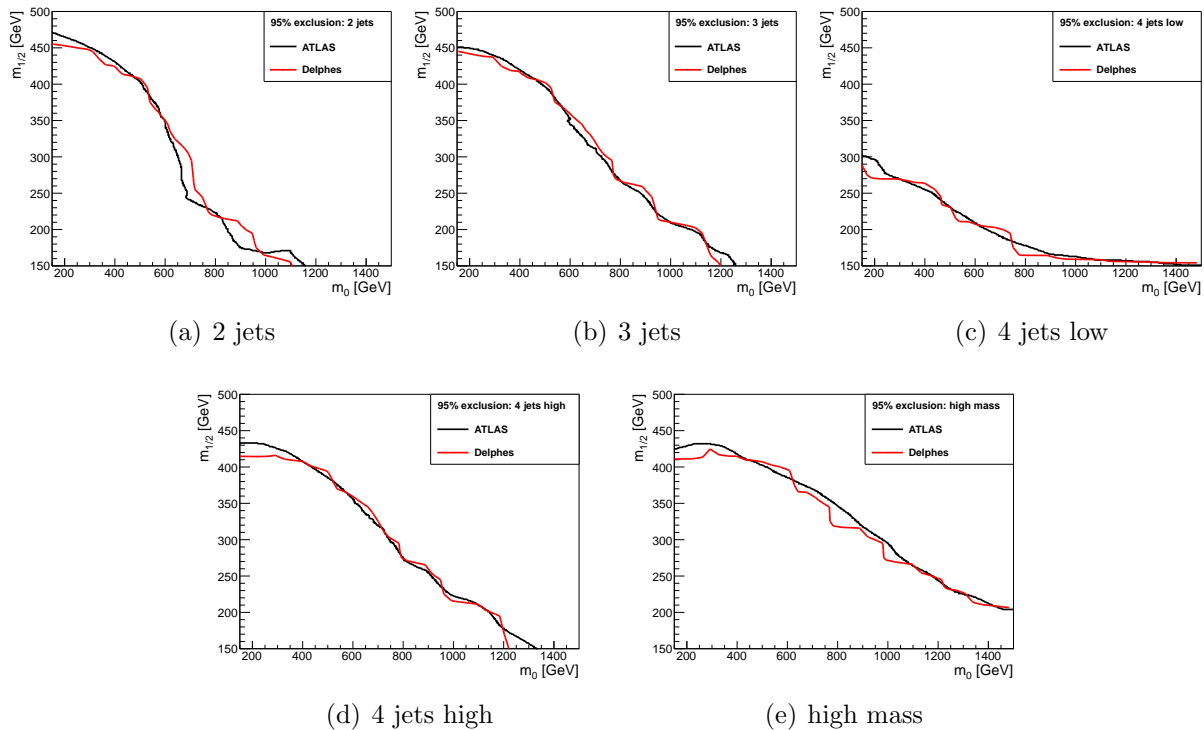


Figure A.1: Comparison of our 95% exclusion contours with those of ATLAS' in the  $\tan\beta = 10$ ,  $A_0 = 0$ ,  $\mu > 0$  slice of the CMSSM for the 0-lepton search.

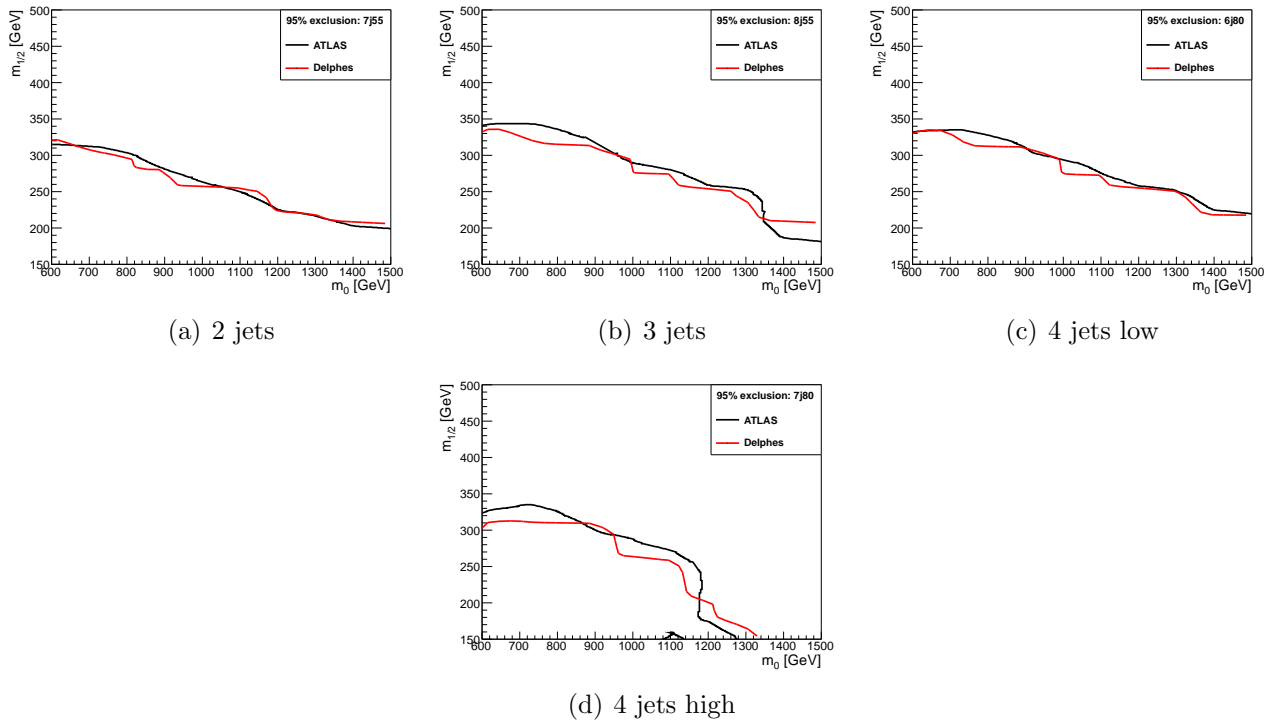


Figure A.2: Comparison of our 95% exclusion contours with those of ATLAS' in the  $\tan \beta = 10$ ,  $A_0 = 0$ ,  $\mu > 0$  slice of the CMSSM for the multijet search.

## References

- [1] L. J. Hall, R. Rattazzi, U. Sarid, Phys. Rev. **D50** (1994) 7048-7065. [hep-ph/9306309].
- [2] M. S. Carena, M. Olechowski, S. Pokorski, C. E. M. Wagner, Nucl. Phys. **B426** (1994) 269-300. [hep-ph/9402253].
- [3] D. M. Pierce, J. A. Bagger, K. T. Matchev, R. -j. Zhang, Nucl. Phys. **B491** (1997) 3-67. [hep-ph/9606211].
- [4] G. D'Ambrosio, G. F. Giudice, G. Isidori and A. Strumia, Nucl. Phys. B **645** (2002) 155 [hep-ph/0207036].
- [5] C. Bobeth, T. Ewerth, F. Kruger and J. Urban, Phys. Rev. D **66** (2002) 074021 [hep-ph/0204225].
- [6] M. Olechowski, S. Pokorski, Phys. Lett. **B344** (1995) 201-210. [hep-ph/9407404].
- [7] Y. Kawamura, H. Murayama, M. Yamaguchi, Phys. Rev. **D51** (1995) 1337-1352. [hep-ph/9406245].

- [8] H. Murayama, M. Olechowski, S. Pokorski, Phys. Lett. **B371** (1996) 57-64. [hep-ph/9510327].
- [9] H. Baer, M. A. Diaz, J. Ferrandis, X. Tata, Phys. Rev. **D61** (2000) 111701. [hep-ph/9907211]; H. Baer, M. Brhlik, M. A. Diaz, J. Ferrandis, P. Mercadante, P. Quintana, X. Tata, Phys. Rev. **D63** (2000) 015007. [hep-ph/0005027].
- [10] T. Blazek, R. Dermisek, S. Raby, Phys. Rev. **D65** (2002) 115004. [hep-ph/0201081]; D. Auto, H. Baer, C. Balazs, A. Belyaev, J. Ferrandis, X. Tata, JHEP **0306** (2003) 023. [hep-ph/0302155]; H. Baer, S. Kraml, S. Sekmen, H. Summy, JHEP **0803** (2008) 056. [arXiv:0801.1831 [hep-ph]].
- [11] H. Baer, S. Kraml, S. Sekmen, JHEP **0909** (2009) 005. [arXiv:0908.0134 [hep-ph]].
- [12] W. Altmannshofer, D. Guadagnoli, S. Raby and D. M. Straub, Phys. Lett. B **668** (2008) 385 [arXiv:0801.4363 [hep-ph]];  
S. Raby, <http://www.bctp.uni-bonn.de/bethe-forum/talks/Raby-BF11.pdf>, talk given at Bethe Forum, Bonn, Germany, 2-18 November 2011.
- [13] CMS and LHCb Collaborations, CMS-PAS-BPH-11-019, LHCb-CONF-2011-047, CERN-LHCb-CONF-2011-047.
- [14] H. Baer, S. Kraml, A. Lessa and S. Sekmen, JHEP **1002** (2010) 055 [arXiv:0911.4739 [hep-ph]].
- [15] ATLAS collaboration, ATLAS-CONF-2011-098.
- [16] M. Badziak, to appear in Mod. Phys. Lett. A.
- [17] M. Badziak, M. Olechowski and S. Pokorski, JHEP **1108** (2011) 147 [arXiv:1107.2764 [hep-ph]].
- [18] S. P. Martin, Phys. Rev. **D79** (2009) 095019. [arXiv:0903.3568 [hep-ph]].
- [19] U. Chattopadhyay and P. Nath, Phys. Rev. D **65** (2002) 075009 [arXiv:hep-ph/0110341].
- [20] M. J. Dolan, D. Grellscheid, J. Jaeckel, V. V. Khoze and P. Richardson, JHEP **1106** (2011) 095 [arXiv:1104.0585 [hep-ph]].
- [21] Y. Kats, P. Meade, M. Reece and D. Shih, arXiv:1110.6444 [hep-ph].
- [22] B. C. Allanach, T. J. Khoo and K. Sakurai, JHEP **1111** (2011) 132 [arXiv:1110.1119 [hep-ph]].
- [23] S. Sekmen, S. Kraml, J. Lykken, F. Moortgat, S. Padhi, L. Pape, M. Pierini and H. B. Prosper *et al.*, arXiv:1109.5119 [hep-ph].

- [24] A. Arbey, M. Battaglia and F. Mahmoudi, arXiv:1110.3726 [hep-ph].
- [25] T. J. LeCompte and S. P. Martin, Phys. Rev. D **84** (2011) 015004 [arXiv:1105.4304 [hep-ph]]; T. J. LeCompte and S. P. Martin, arXiv:1111.6897 [hep-ph].
- [26] K. Sakurai and K. Takayama, JHEP **1112** (2011) 063 [arXiv:1106.3794 [hep-ph]].
- [27] M. Papucci, J. T. Ruderman and A. Weiler, arXiv:1110.6926 [hep-ph].
- [28] C. Brust, A. Katz, S. Lawrence and R. Sundrum, arXiv:1110.6670 [hep-ph].
- [29] R. Essig, E. Izaguirre, J. Kaplan and J. G. Wacker, arXiv:1110.6443 [hep-ph].
- [30] N. Desai and B. Mukhopadhyaya, arXiv:1111.2830 [hep-ph].
- [31] I. Gogoladze, R. Khalid, S. Raza, Q. Shafi, JHEP **1012** (2010) 055. [arXiv:1008.2765 [hep-ph]]; I. Gogoladze, R. Khalid and Q. Shafi, Phys. Rev. D **79** (2009) 115004 [arXiv:0903.5204 [hep-ph]].
- [32] M. A. Ajaib, T. Li and Q. Shafi, Phys. Lett. B **705** (2011) 87 [arXiv:1107.2573 [hep-ph]].
- [33] G. Aad *et al.* [ATLAS Collaboration], arXiv:1109.6572 [hep-ex].
- [34] G. Aad *et al.* [Atlas Collaboration], JHEP **1111** (2011) 099 [arXiv:1110.2299 [hep-ex]].
- [35] I. Gogoladze, Q. Shafi and C. S. Un, arXiv:1112.2206 [hep-ph].
- [36] I. Gogoladze, Q. Shafi and C. S. Un, Phys. Lett. B **704** (2011) 201 [arXiv:1107.1228 [hep-ph]].
- [37] E. Komatsu *et al.* [WMAP Collaboration], Astrophys. J. Suppl. **192** (2011) 18 [arXiv:1001.4538 [astro-ph.CO]].
- [38] V. M. Abazov *et al.* [D0 Collaboration], Phys. Lett. B **693** (2010) 95 [arXiv:1005.2222 [hep-ex]].
- [39] ATLAS collaboration, ATLAS-CONF-2011-132.
- [40] CMS collaboration, CMS-HIG-11-020.
- [41] S. Gennai, S. Heinemeyer, A. Kalinowski, R. Kinnunen, S. Lehti, A. Nikitenko and G. Weiglein, Eur. Phys. J. C **52** (2007) 383 [arXiv:0704.0619 [hep-ph]].
- [42] B. C. Allanach, Comput. Phys. Commun. **143** (2002) 305-331. [hep-ph/0104145].
- [43] A. Djouadi, M. M. Muhlleitner and M. Spira, Acta Phys. Polon. B **38** (2007) 635 [hep-ph/0609292]; A. Djouadi, J. Kalinowski and M. Spira, Comput. Phys. Commun. **108** (1998) 56 [hep-ph/9704448]; M. Muhlleitner, A. Djouadi and Y. Mambrini, Comput. Phys. Commun. **168** (2005) 46 [hep-ph/0311167].

- [44] M. Bahr, S. Gieseke, M. A. Gigg, D. Grellscheid, K. Hamilton, O. Latunde-Dada, S. Platzer and P. Richardson *et al.*, Eur. Phys. J. C **58** (2008) 639 [arXiv:0803.0883 [hep-ph]].
- [45] S. Ovyn, X. Rouby and V. Lemaitre, arXiv:0903.2225 [hep-ph].
- [46] W. Beenakker, R. Hopker, M. Spira and P. M. Zerwas, Nucl. Phys. B **492** (1997) 51 [arXiv:hep-ph/9610490]; W. Beenakker, M. Kramer, T. Plehn, M. Spira and P. M. Zerwas, Nucl. Phys. B **515** (1998) 3 [arXiv:hep-ph/9710451]; M. Spira, arXiv:hep-ph/0211145; T. Plehn, Czech. J. Phys. **55** (2005) B213 [arXiv:hep-ph/0410063].
- [47] A. L. Read, J. Phys. GG **28** (2002) 2693.
- [48] B. C. Allanach, T. J. Khoo, C. G. Lester and S. L. Williams, JHEP **1106** (2011) 035 [arXiv:1103.0969 [hep-ph]].
- [49] P. M. Nadolsky, H. -L. Lai, Q. -H. Cao, J. Huston, J. Pumplin, D. Stump, W. -K. Tung and C. -P. Yuan, Phys. Rev. D **78** (2008) 013004 [arXiv:0802.0007 [hep-ph]].
- [50] G. Belanger, F. Boudjema, A. Pukhov, A. Semenov, Comput. Phys. Commun. **176** (2007) 367-382. [hep-ph/0607059].
- [51] G. W. Bennett *et al.* [ Muon G-2 Collaboration ], Phys. Rev. **D73** (2006) 072003. [hep-ex/0602035]; M. Davier, A. Hoecker, B. Malaescu, Z. Zhang, Eur. Phys. J. **C71** (2011) 1515. [arXiv:1010.4180 [hep-ph]].
- [52] D. Asner *et al.* [Heavy Flavor Averaging Group], arXiv:1010.1589 [hep-ex]; M. Misiak, H. M. Asatrian, K. Bieri, M. Czakon, A. Czarnecki, T. Ewerth, A. Ferroglia, P. Gambino *et al.*, Phys. Rev. Lett. **98** (2007) 022002. [hep-ph/0609232]; G. Degrossi, P. Gambino and G. F. Giudice, JHEP **0012** (2000) 009 [arXiv:hep-ph/0009337].
- [53] S. Schael *et al.* [ALEPH Collaboration and DELPHI Collaboration and L3 Collaboration and ], Eur. Phys. J. C **47** (2006) 547 [arXiv:hep-ex/0602042].
- [54] B. C. Allanach, A. Djouadi, J. L. Kneur, W. Porod and P. Slavich, JHEP **0409** (2004) 044 [arXiv:hep-ph/0406166].
- [55] ATLAS Collaboration, arXiv:1112.3832 [hep-ex].